



# Efficiency of Iron- and Calcium-Impregnated Biochar in Adsorbing Phosphate From Wastewater in Onsite Wastewater Treatment Systems

Sahar S. Dalahmeh<sup>1,2\*</sup>, Ylva Stenström<sup>1</sup>, Mohamed Jebrane<sup>3</sup>, Lars D. Hylander<sup>1</sup>, Geoffrey Daniel<sup>3</sup> and Ivo Heinmaa<sup>4</sup>

<sup>1</sup> Department of Energy and Technology, Swedish University of Agricultural Sciences, Uppsala, Sweden, <sup>2</sup> Department of Earth Sciences, Uppsala University, Uppsala, Sweden, <sup>3</sup> Department of Forest Biomaterials and Technology/Wood Science, Swedish University of Agricultural Sciences, Uppsala, Sweden, <sup>4</sup> National Institute of Chemical Physics and Biophysics, Tallinn, Estonia

## OPEN ACCESS

### Edited by:

Alberto Tiraferrì,  
Politecnico di Torino, Italy

### Reviewed by:

Xiaofei Tan,  
Hunan University, China  
Konstantinos Plakas,  
Centre for Research and Technology  
Hellas (CERTH), Greece

### \*Correspondence:

Sahar S. Dalahmeh  
sahar.dalahmeh@slu.se;  
sahar.dalahmeh@geo.uu.se

### Specialty section:

This article was submitted to  
Water and Wastewater Management,  
a section of the journal  
Frontiers in Environmental Science

**Received:** 13 March 2020

**Accepted:** 20 October 2020

**Published:** 20 November 2020

### Citation:

Dalahmeh SS, Stenström Y,  
Jebrane M, Hylander LD, Daniel G  
and Heinmaa I (2020) Efficiency  
of Iron- and Calcium-Impregnated  
Biochar in Adsorbing Phosphate  
From Wastewater in Onsite  
Wastewater Treatment Systems.  
*Front. Environ. Sci.* 8:538539.  
doi: 10.3389/fenvs.2020.538539

This study evaluated the potential of biochar impregnated with Fe<sup>3+</sup> or Ca<sup>2+</sup>, or mixed with Polonite®, as a filter material for removal of phosphate (PO<sub>4</sub>-P) from wastewater in onsite wastewater treatment systems (OWTS). Four treatments with biochar were investigated: unimpregnated biochar (UBC), biochar impregnated with iron Fe<sup>3+</sup> (FBC), biochar impregnated with calcium oxide (CBC), and biochar mixed with Polonite® (PBC). In a batch experiment using phosphate solution at concentrations 0.5, 3.3, 6.5, 13, and 26 mg PO<sub>4</sub>-P L<sup>-1</sup>, adsorption of PO<sub>4</sub>-P in the different treatments was modeled using Langmuir and Freundlich isotherms. Column filters (5 diameter × 55 cm height) packed with UBC, FBC, CBC, and PBC were then furnished with raw wastewater over 148 weeks. During this experiment, adsorption of PO<sub>4</sub>-P was investigated in response to increasing hydraulic loading rate (HLR; 56, 74, and 112 L m<sup>-2</sup> day<sup>-1</sup>) and increasing phosphate loading rate (PLR; 195, 324, 653, and 1715 mg PO<sub>4</sub>-P m<sup>-2</sup> day<sup>-1</sup>). Among the materials, FBC had the highest maximum adsorption capacity (Q<sub>m</sub>) based on Langmuir isotherms (3.21 ± 0.01 mg g<sup>-1</sup>). FBC and CBC showed robust performance with increasing HLR, while increasing PLR increased the amount of PO<sub>4</sub>-P retained in all filters. After 148 weeks of operation, removal of PO<sub>4</sub>-P (averaged over the last 18 weeks of operation) was 13 ± 16% for UBC, 40 ± 20% for CBC, 88 ± 12% for FBC, and 30 ± 18% for PBC. The PO<sub>4</sub>-P amount retained in filters over the 148 weeks was 84.75, 221.75, 358.38, and 152.36 g m<sup>-2</sup> in UBC, CBC, FBC, and PBC, respectively. The adsorption capacity of the filters after 148 weeks was 1.50, 4.02, 6.41, and 2.75 mg g<sup>-1</sup> for UBC, CBC, FBC, and PBC, respectively. The adsorption capacity values and breakthrough curves showed that low concentrations (i.e., <2.6 mg L<sup>-1</sup>) of PO<sub>4</sub>-P in wastewater would allow the FBC filter to remain active for 58 months and the CBC filter for 15 months, before PO<sub>4</sub>-P removal declined to <70%. In conclusion, biochar impregnated with iron and calcium is a promising solution for removal of PO<sub>4</sub>-P from wastewater in OWTS.

**Keywords:** adsorption, biochar, iron impregnation, calcium impregnation, onsite wastewater treatment, phosphate retention

## INTRODUCTION

Wastewater discharge and agricultural runoff are major contributors to anthropogenic phosphorus (P) discharge to many inland aquatic systems worldwide (Smith, 2003). Agricultural activities and wastewater effluents account for the majority of annual P discharge to water bodies (HELCOM, 2018; Schellenger and Hellweger, 2019). In industrialized countries (e.g., Sweden), there are stringent requirements that regulate the quality of wastewater effluents in small scale and onsite systems in order to protect water bodies, and high-technology solutions are often used for additional P removal from wastewater to meet the environmental regulations (Havss och vattenmyndighetens, 2016). However, wastewater quality from small-scale onsite wastewater systems (OWTS) is poor in terms of P removal (Heinonen-Tanski and Matikka, 2017), although the anthropogenic P load from OWTS is still smaller than the agricultural load. However, onsite systems can still be a relevant P source, especially in areas such as the Baltic Sea Region where reducing P loads in water bodies is high priority (Heinonen-Tanski and Matikka, 2017; HELCOM, 2018).

One environmentally friendly and effective treatment method for onsite wastewater treatment is the use of biochar filters. Biochar is produced by heating biomass at high temperature (300–800°C) in limited presence of oxygen (Downie et al., 2009), and is characterized by large specific surface and high porosity. Organic materials such as agricultural waste, sewage sludge and forest residues can act as a resource for biochar production, thereby contributing to sustainable management and re-utilization of waste products (He et al., 2016). Previous studies have demonstrated the efficiency of biochar in removing organic matter, surfactants, and nitrogen (N) from wastewater and graywater (Berger, 2012; Niwagaba et al., 2014; Dalahmeh, 2016). However, removal of P by biochar was not efficient in the latter studies, and there is therefore a need to investigate whether modification of the biochar surface by impregnating with iron (Fe) and calcium (Ca) would enhance the capacity for P removal. Modification of the surface of biochar by impregnation with different cations has been investigated previously to some extent. For example, He et al. (2017) investigated nanocomposites of iron oxide (Fe<sub>3</sub>O<sub>4</sub>) biochar for removal of different pollutants, including PO<sub>4</sub>, from wastewater. They found that Fe<sub>3</sub>O<sub>4</sub>/biochar nanocomposites not only showed significantly enhanced PO<sub>4</sub><sup>3-</sup> removal (100%), but also significantly shortened the time needed for complete removal. In a study by Chen et al. (2011), biochar powder for P removal was produced at different temperatures and impregnated with magnetite (Fe<sub>2</sub>O<sub>3</sub>) with a biochar to Fe ratio of 0.9. The modified biochar showed higher P adsorption (up to 99% removal) than unmodified control biochar. Adding iron oxides to biochar can also have structural benefits, producing larger pore volume and specific surface area (Ren et al., 2015). Ferric chloride (FeCl<sub>3</sub>) biochar was studied by Li et al. (2016), who found that an Fe to biochar ratio of 0.7 resulted in P adsorption of up to 16.58 mg g<sup>-1</sup> biochar, compared with less than 1 mg g<sup>-1</sup> in natural sand (Del Bubba et al., 2003). In a study testing column filters with Fe-modified biochar, Liu et al. (2012) found that 99% of the total P concentration

was removed. Jung et al. (2016) analyzed fine biochar material produced by algae (as dried calcium-alginate beads) and found it had a capacity to remove 100 mg P g<sup>-1</sup> biochar. However all these studies evaluated the performance of biochar in batch experiments and P adsorption by impregnated biochar from real wastewater was not investigated. Additionally, the performance of impregnated biochar in unsaturated column filters over extended periods and under different loading conditions was not investigated.

The main objective of the present study was to evaluate the potential of biochar impregnated with Fe<sup>3+</sup> or Ca<sup>2+</sup>, or mixed with Polonite, as filter material for adsorption of PO<sub>4</sub>-P in OWTS. Specific objectives were to (i) determine the adsorption isotherm of PO<sub>4</sub>-P in biochar impregnated with Fe, biochar impregnated with Ca, and biochar mixed with Polonite in batch adsorption experiments, and (ii) demonstrate and assess the performance of impregnated biochar filters in PO<sub>4</sub>-P removal from wastewater under different hydraulic loading rates (HLR) and phosphate loading rates (PLR) in column experiments.

## MATERIALS AND METHODS

### Biochar Preparation

Four treatments with biochar were tested: (i) unimpregnated biochar (UBC); (ii) biochar impregnated with calcium oxide (CaO; CBC); biochar impregnated with FeCl<sub>3</sub> (FBC) and biochar mixed with Polonite® (PBC). For treatments FBC and CBC, pine bark (Rimbo Jord, Stockholm) of grain size 1–5 mm was soaked in FeCl<sub>3</sub> solution (purity 97%; VWR, Stockholm) and CaO (purity 95%; VWR, Stockholm), respectively, before pyrolysis. The FeCl<sub>3</sub> or CaO to bark ratio was 0.3 on a dry matter (DM) basis. After being mixed in the solution for 24 h in room temperature, the impregnated bark was dried at 100°C for another 24 h. Finally, the dried biomass was charred in a muffle stove at 350–400°C for 3.5 h according to Agrafioti et al. (2014). UBC was produced by pyrolysis of similar pine bark without impregnation. For treatment PBC, after pyrolysis, UBC was mixed with Polonite® gravel with a Polonite/biochar DM ratio of 0.3. Polonite® is a commercially available and reactive material which is used for phosphorus adsorption. It is produced by heating opoka rock to 900°C that results in transforming CaCO<sub>3</sub> to the more reactive CaO (Renman and Renman, 2010). The Polonite® used in the current experiment had particle size of 1–3 mm and it was obtained from Ecofiltration Nordic AB (Stockholm, Sweden).

### Batch Adsorption Experiments

A batch experiment was carried out to assess and compare the P adsorption capacity of the different biochars (UBC, FBC, CBC, and PBC). For this, 1 g samples of biochar were added to 500 mL conical flasks containing 100 mL of PO<sub>4</sub>-P solution with concentrations 0.5, 3.3, 6.5, 13, and 26 mg PO<sub>4</sub>-P L<sup>-1</sup>, respectively. The concentrations were prepared by diluting 1000 mg PO<sub>4</sub> L<sup>-1</sup> stock solution based on monopotassium phosphate (KH<sub>2</sub>PO<sub>4</sub>; VWR, Stockholm) with distilled water. The PO<sub>4</sub>-P concentrations were selected based on those expected in

an OWTS, and diluted according to Palm et al. (2002). Three replicates ( $n = 3$ ) were prepared for each concentration and each treatment except the  $0.5 \text{ mg PO}_4\text{-P L}^{-1}$  concentration, which only had one replicate ( $n = 1$ ). The flasks were shaken on a rotary table for 24 h at 130 rpm and controlled room temperature of  $20 \pm 2^\circ\text{C}$ . Samples (6 mL) were taken from each flask after 0 min, 15 min, 75 min, 4 h, and 24 h, using a pipette. Collected samples were filtered through a  $0.45 \mu\text{m}$  filter and their pH and  $\text{PO}_4\text{-P}$  concentration determined. After 24 h, the residual solids were washed with deionized water, oven-dried at  $80^\circ\text{C}$  for 4 h, and stored in the freezer for further characterization.

## Column Filter Experiments

In the column filter experiments, acrylic columns were used as filters to study the removal of chemical oxygen demand (COD), and  $\text{PO}_4\text{-P}$  from wastewater. The columns (60 cm high, 5 cm diameter) were packed separately with biochar (UBC, PBC, CBC, or FBC) to form a layer of 50 cm. Single columns were prepared for each material. A 5 cm layer of coarse biochar (8–15 mm in particle size) was placed on the top and bottom of the filters to prevent clogging and to facilitate drainage (Figure 1).

## Loading Conditions for the Column Filters

The column filters were tested for removal of  $\text{PO}_4\text{-P}$  over an operating period from October 2016 to August 2019. During this period, the performance of filters in terms of pollutant removal was investigated in response to different HLR and PLR, as described below.

### Hydraulic Loading Rate Trial

The removal of  $\text{PO}_4\text{-P}$  and COD from wastewater was investigated in response to changing hydraulic loading conditions. During this trial, the filters were operated with an HLR of  $56 \text{ L m}^{-2} \text{ day}^{-1}$  for 33 weeks (including the start-up period),  $74 \text{ L m}^{-2} \text{ day}^{-1}$  for a further 30 weeks, and  $112 \text{ L m}^{-2} \text{ day}^{-1}$  for 10 weeks. The filters were fed with wastewater at the planned HLR, without modifying the concentrations of organic matter, N, or P of the wastewater. The concentrations of  $\text{PO}_4\text{-P}$  and the organic loading rate (OLR) and PLR applied during the HLR trial are summarized in Table 1.

### Phosphate Loading Rate Trial

The removal of  $\text{PO}_4\text{-P}$  and COD in response to changing PLR was investigated by exposing the filters to stepwise increasing PLR while the HLR was kept unchanged at  $74 \text{ L m}^{-2} \text{ day}^{-1}$  (Table 2). During this trial, the filters received  $194 \pm 65 \text{ mg PO}_4\text{-P m}^{-2} \text{ day}^{-1}$  for 18 weeks,  $324 \pm 27 \text{ mg PO}_4\text{-P m}^{-2} \text{ day}^{-1}$  for 23 weeks,  $653 \pm 61 \text{ mg PO}_4\text{-P m}^{-2} \text{ day}^{-1}$  for 13 weeks, and  $1715 \pm 39 \text{ mg PO}_4\text{-P m}^{-2} \text{ day}^{-1}$  for 18 weeks. The  $\text{PO}_4\text{-P}$  concentration was modified to give the target PLR by adding 15, 30, 90, and 150 mL of  $\text{PO}_4$  standard solution ( $1000 \text{ mg L}^{-1}$ ) to 1 L raw wastewater. The  $\text{PO}_4\text{-P}$  concentration in the raw wastewater was  $2.6 \pm 0.86 \text{ mg L}^{-1}$ . Concentrations of all other components in the raw wastewater were not modified during this trial. Inflow characteristics, HLR, OLR, and PLR of the feed wastewater during this trial are summarized in Table 2.

## Preparation, Storage, and Dosage of Wastewater

All column filters were fed with raw wastewater in single-pass unsaturated downflow mode. The raw wastewater was obtained from Uppsala wastewater treatment plant (Kungsängsverket) on a weekly basis. When needed (i.e., during the PLR trial), the concentration of  $\text{PO}_4\text{-P}$  was changed. The wastewater was cooled in a fridge ( $4 \pm 2^\circ\text{C}$ ) when brought from Kungsängsverket. Before each dosage, the cooled wastewater was mixed by homogenization and the required dosage pumped from the refrigerated container to distribution containers placed at room temperature ( $20^\circ\text{C}$ ). After reaching room temperature, the wastewater doses were pumped from the distribution containers to the filters, using a peristaltic pump.

## Chemical Analysis

The inflow wastewater and effluents from the different filters were analyzed to determine the pH, electrical conductivity (EC), COD, and  $\text{PO}_4\text{-P}$ . The pH was measured using a WTW pH/ion 340i meter and EC using a Condi 330i conductivity meter (WTW, Weilheim, Germany). The COD and  $\text{PO}_4\text{-P}$  concentrations were determined using Spectroquant® cell kits (numbers 14772–14773 (COD) and 14543 ( $\text{PO}_4\text{-P}$ ), Merck KGaA, Darmstadt, Germany). Concentrations were determined colorimetrically using a Nova 60 photometer (Merck KGaA).

## Characterization of Biochar

Chemical composition of surface, particle shape, topography, and functional groups on the different biochars (UBC, PBC, CBC, and FBC) were characterized using Fourier transform infrared (FTIR), X-ray diffraction (XRD), and scanning electron microscopy (SEM). Infrared absorption spectra of the biochar samples were obtained using a Spectrum Two FTIR (Perkin-Elmer) equipped with an UATR Diamond accessory, according to Jebrane et al. (2017). The XRD patterns were obtained by a PANalytical B.V. X'Pert3 Powder diffractometer (Netherlands) with Cu-K $\alpha$  radiation ( $k = 1.54059 \text{ \AA}$ ) within angular range of  $2\theta = 5\text{--}70^\circ$  at  $25^\circ\text{C}$ . SEM was used to observe the surface morphology of the impregnated biochars. Biochar samples were deposited on stubs bearing double-sided tape and coated with a  $\sim 6 \text{ nm}$  layer of gold using an Emitech K550X sputter coater. Samples were observed using a Philips XL30 ESEM operated at variable kV. Images were digitalized using the microscope software.

## Calculations of Adsorption Isotherms

Removal efficiency ( $E$ ) was calculated from the difference in concentration between inflow and outflow of the filters as:

$$E = 100 \frac{C_{in} - C_{out}}{C_{in}} \quad (1)$$

where  $E$  is the removal efficiency (%),  $C_{in}$  is the concentration in the inflow ( $\text{mg L}^{-1}$ ), and  $C_{out}$  is the concentration in outflow ( $\text{mg L}^{-1}$ ).

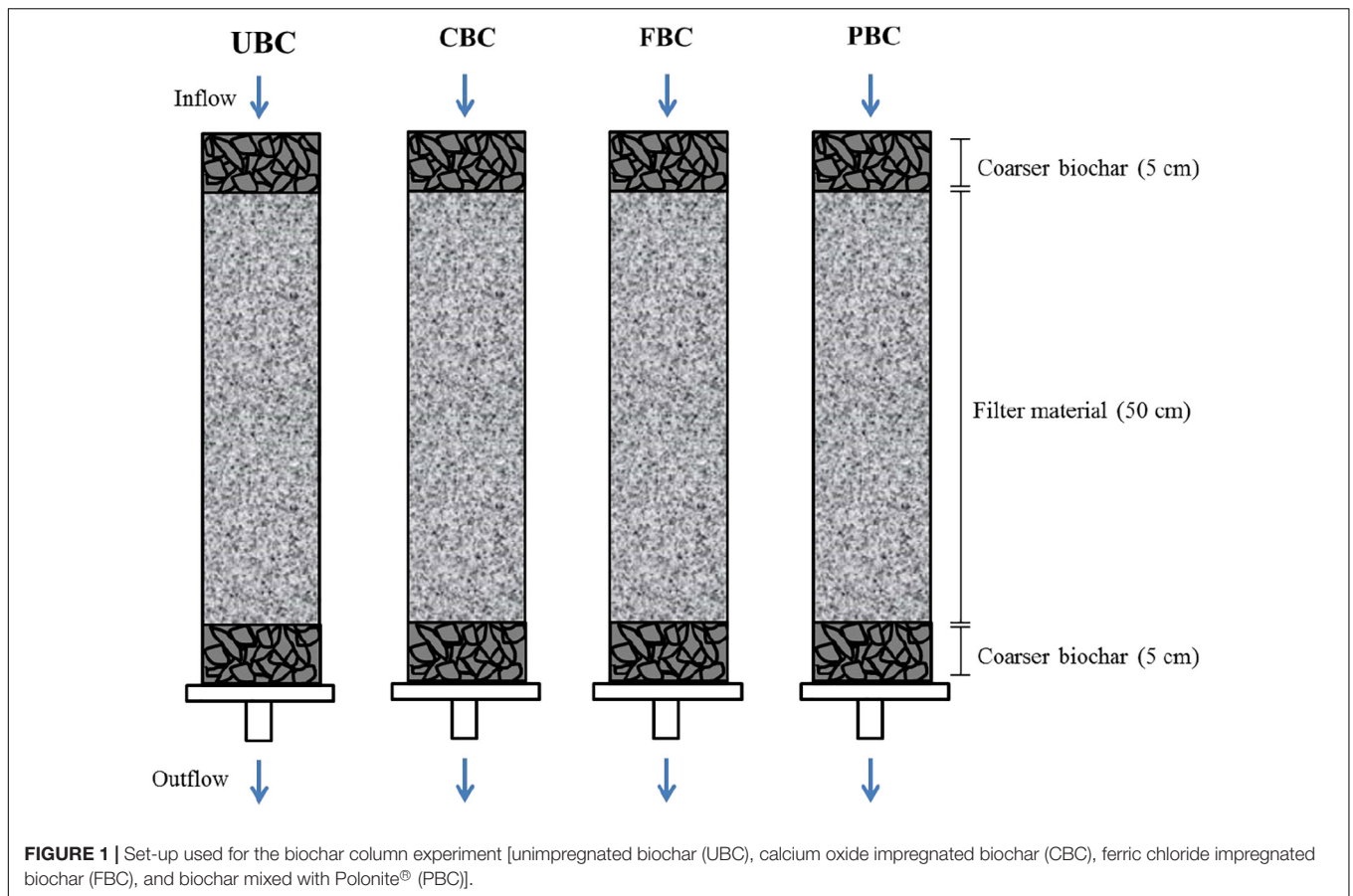


**TABLE 1** | Loading conditions used during the hydraulic loading rate (HLR) trial.

ID	HLR (L m <sup>-2</sup> day <sup>-1</sup> )	Duration (week)	PO <sub>4</sub> -P (mg L <sup>-1</sup> )	OLR (g COD m <sup>-2</sup> day <sup>-1</sup> )	PLR (mg PO <sub>4</sub> -P m <sup>-2</sup> day <sup>-1</sup> )
HLR 56	56 ± 0	33	2.99 ± 1.33	25 ± 11	187 ± 74
HLR74	74 ± 0	30	2.04 ± 1.06	38 ± 29	151 ± 80
HLR112	112 ± 0	10	2.43 ± 1.60	52 ± 15	271 ± 178

OLR, organic loading rate; PLR, phosphate-phosphorus (PO<sub>4</sub>-P) loading rate; COD, chemical oxygen demand. Values shown are mean ± SD.

**TABLE 2** | Loading conditions used during the phosphate loading trial.

ID	PLR (mg PO <sub>4</sub> -P m <sup>-2</sup> day <sup>-1</sup> )	Duration (week)	PO <sub>4</sub> -P (mg L <sup>-1</sup> )	OLR (g COD m <sup>-2</sup> day <sup>-1</sup> )	HLR (L m <sup>-2</sup> day <sup>-1</sup> )
PLR-194	194 ± 64	18	2.60 ± 0.86	26 ± 11	74 ± 0
PLR-324	324 ± 27	23	4.36 ± 0.37	28 ± 8	74 ± 0
PLR-653	653 ± 61	10	8.78 ± 0.82	40 ± 10	74 ± 0
PLR-1715	1715 ± 39	18	23.04 ± 0.53	40 ± 4	74 ± 0

PLR, phosphate-phosphorus (PO<sub>4</sub>-P) loading rate; OLR, organic loading rate; HLR, hydraulic loading rate; COD, chemical oxygen demand. Values shown are mean ± SD.

Adsorption of phosphate (Q) in the batch adsorption experiment was calculated as:

$$Q = (C_0 - C_e) \times \frac{V}{m} \quad (2)$$

where Q is mg P adsorbed per g biochar (mg g<sup>-1</sup>), C<sub>0</sub> is the initial concentration of solution (mg L<sup>-1</sup>), C<sub>e</sub> is the concentration

(mg L<sup>-1</sup>) after 24 h in the batch equilibrium experiment, V is the volume of solution (100 mL), and m the mass of adsorbent (1 g).

Langmuir and Freundlich adsorption isotherms were modeled for each biochar type. Langmuir isotherms were calculated according to Mead (1981):

$$Q_e = \frac{k_L Q_m C_e}{1 + k_L C_e} \quad (3)$$

where  $Q_e$  ( $\text{mg g}^{-1}$ ) is the equilibrium adsorption capacity,  $C_e$  ( $\text{mg L}^{-1}$ ) is the concentration at equilibrium,  $k_L$  ( $\text{L mg}^{-1}$ ) is the Langmuir adsorption constant, and  $Q_m$  ( $\text{mg g}^{-1}$ ) is the maximum adsorption capacity.

Freundlich isotherms were calculated as:

$$Q_e = k_F C_e^{1/n} \quad (4)$$

where  $k_F$  ( $\text{L g}^{-1}$ ) is the Freundlich constant and  $n$  is the dimensionless Freundlich heterogeneity exponent.

## RESULTS

### Characteristics of Biochar

#### FTIR Analysis and SEM

The FTIR spectra of FBC, CBC, PBC, and UBC are shown in Figure 2. The peaks observed in the region  $1800\text{--}650\text{ cm}^{-1}$  in all spectra were attributed to carbonyl stretching vibrations and to  $\text{-COOH}$  symmetric stretching vibrations. The band observed around  $780\text{ cm}^{-1}$  could be attributable to in-plane and out-of-plane C-H bends. The  $\text{FeCl}_3$ -impregnated (FBC) filter (freshly prepared before use in wastewater treatment) caused only a slight change in the spectrum, mainly around  $650\text{ cm}^{-1}$ , where a new peak most probably attributable to iron oxalate was observed. In addition, a decrease in the peak around  $1020\text{ cm}^{-1}$  was observed, probably as a result of shifting from  $\text{COOH}$  to  $\text{COO}^-$ . After using the FBC filter for wastewater treatment, no significant changes were observed except disappearance of the peak at around  $650\text{ cm}^{-1}$  characteristic of iron oxalate, possibly due to leaching of iron from the filters. The FTIR spectrum of the fresh CBC filter showed emergence of new characteristic absorption bands around  $1410$ ,  $1315$ ,  $874$ , and  $780\text{ cm}^{-1}$  which could be attributed to C-O and Ca-O bonds. After use of CBC for wastewater treatment, a slight decrease in the intensity of the C-O and Ca-O peaks was observed due to phosphate adsorption and interaction with the impregnated calcium oxide species. The FTIR spectrum of the fresh Polonite filter (PCB) exhibited strong absorption bands at  $1410$  and  $870\text{ cm}^{-1}$ , which are characteristic bands of carbonate anions, and other peaks around  $1080$ ,  $980$ ,  $944$ , and  $712\text{ cm}^{-1}$ , which were attributed to the vibrations of wollastonite ( $\beta\text{-CaSiO}_3$ ). A small peak observed at  $3640\text{ cm}^{-1}$  was attributed to water vibrations (Figure 2). After PCB was used for wastewater treatment, a significant decrease in the carbonate anion band intensity was observed, suggesting formation of phosphate complexes. For untreated biochar (UBC), there were no significant peaks in the FTIR spectra. The surface shape and topography of the UBC, CBC, FBC, and PBC materials are shown by SEM images in Supplementary Figure S1.

#### XRD Analysis

Untreated biochar contained 56% quartz, 27% albite, and 17% microcline (Table 3 and Supplementary Figures S2, S3). Impregnation of biochar with CaO resulted in a decrease in the quartz content, disappearance of microcline and albite, and formation of calcite (54%), while impregnation with  $\text{FeCl}_3$  resulted in reduction in quartz content, a slight increase in albite,

and formation of akaganeite (32%). Virgin Polonite contains 52% quartz, 25% calcite, and 23% wollastonite. After using the untreated and CaO-impregnated biochar for wastewater treatment, no significant changes in the mineral content were observed. After filtration, the  $\text{FeCl}_3$ -impregnated biochar showed a significant decrease in quartz content and slight decrease in akaganeite and albite, with formation of monalbite. The combination of Polonite and biochar used for Tot-P and  $\text{PO}_4\text{-P}$  adsorption showed an increase in quartz content, disappearance of albite, microcline, calcite, and wollastonite, and formation of anorthite and orthoclase.

### Langmuir and Freundlich Adsorption Isotherms in UBC, CBC, FBC, and PBC

FBC had a maximum adsorption capacity ( $Q_m$ ) according to Langmuir isotherms ( $3.21 \pm 0.01\text{ mg g}^{-1}$ ) (Table 4). CBC did not reach equilibrium during the experiment. The maximum  $\text{PO}_4\text{-P}$  concentration investigated for CBC was ( $26.7\text{ mg L}^{-1}$ ) and was totally adsorbed during the adsorption experiment. The Langmuir isotherms had a stronger correlation for UBC and FBC, and the Freundlich isotherms for PBC. Correlation coefficients ( $R^2$ ) were in the range  $0.957\text{--}0.997$  for Langmuir isotherms and  $0.960\text{--}0.993$  for Freundlich isotherms for  $\text{PO}_4\text{-P}$  adsorption to the biochars (Table 4). All adsorption isotherms showed an increase in equilibrium concentration ( $C_e$ ) resulted from an increase in P adsorption on the biochar surface ( $Q_e$ ) (Figure 3).

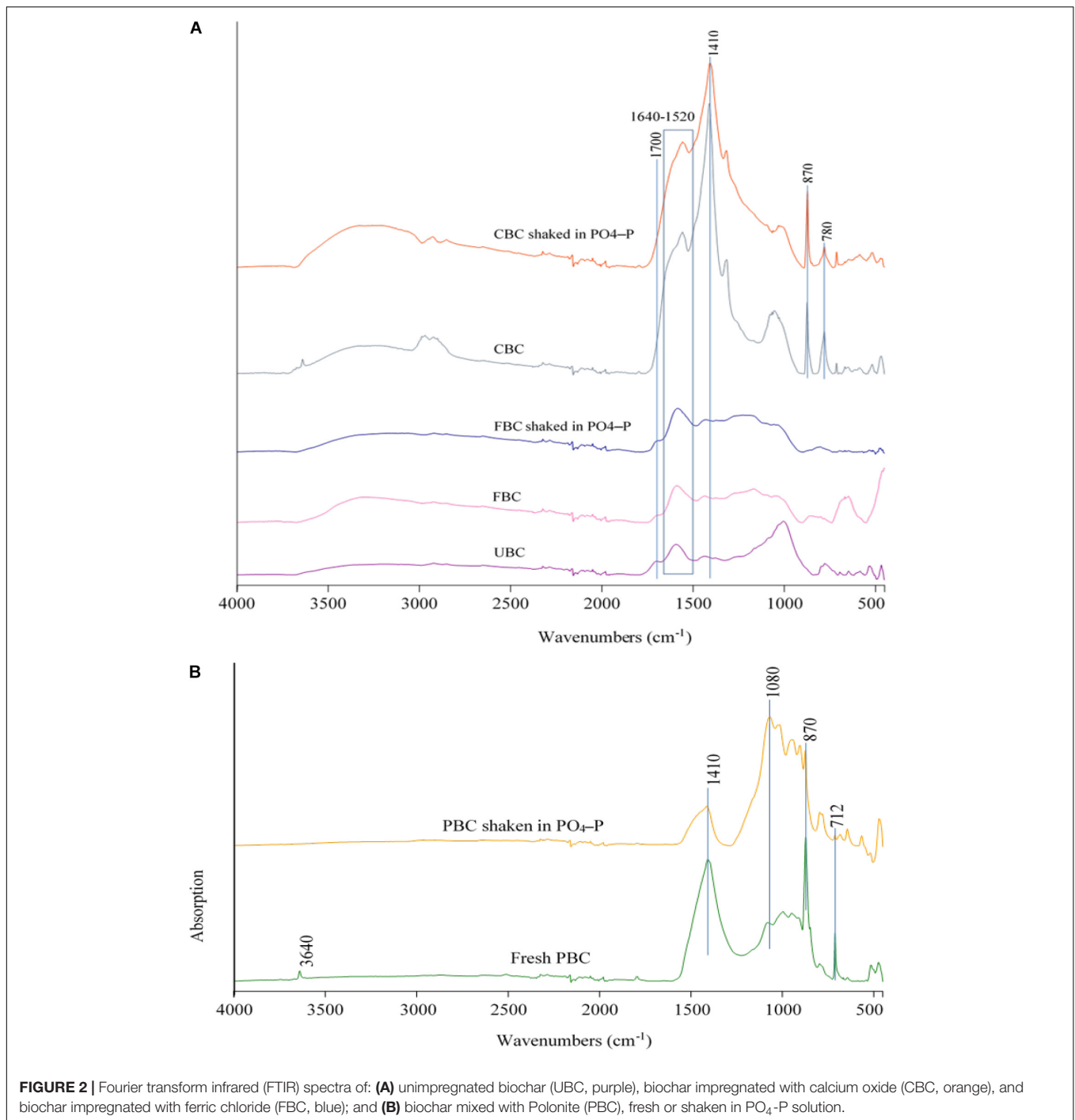
### Adsorption Capacity of Phosphate in UBC, CBC, FBC, and PBC Filters

The  $\text{PO}_4\text{-P}$  adsorption capacity was highest in FBC and lowest in UBC, with the filters following the order  $\text{FBC} > \text{CBC} > \text{PBC} > \text{UBC}$ , with overall  $\text{PO}_4\text{-P}$  adsorption capacity of the different filters  $1.50$ ,  $4.02$ ,  $6.41$ , and  $2.75\text{ mg per g biochar}$  for UBC, CBC, FBC, and PBC, respectively (Figure 4). The corresponding surface removal rate of  $\text{PO}_4\text{-P}$  was  $358.36$ ,  $221.75$ ,  $152.36$ , and  $84.75\text{ g m}^{-2}$  of the filter surface, in the same order. At the end of the operation period of the filter, removal of  $\text{PO}_4\text{-P}$  (averaged over the last 18 weeks of operation) was  $13 \pm 16\%$  for UBC,  $30 \pm 18\%$  for PBC,  $88 \pm 12\%$  for FBC, and  $40 \pm 20\%$  for CBC (Figure 4).

The low removal in UBC (4–6%) of  $\text{PO}_4\text{-P}$  toward the end of the period indicated that UBC may have reached its ultimate  $\text{PO}_4\text{-P}$  retention capacity during the experimental period (148 weeks) (Figures 4B,C). Removal of  $\text{PO}_4\text{-P}$  in CBC (14–23%) and PBC (11–15%) was also low by the end of the experiment. In contrast,  $\text{PO}_4\text{-P}$  removal in the FBC filter declined to almost 63% by the end of the experimental period (week 148).

### Phosphate Removal in Response to Changes in Hydraulic Loading Rate

From the filters tested, FBC showed highest removal of  $\text{PO}_4\text{-P}$  (96%) and was least sensitive to changes in HLR, followed by CBC (77–95% removal) (Figure 5 and Table 5). UBC was least efficient in  $\text{PO}_4\text{-P}$  removal (–9 to 46%) and the least robust to changes in HLR.



With the UBC filter, the average percentage PO<sub>4</sub>-P removal was lower for HLR-74 than HLR-56 and the filter performed best when HLR was 112 L m<sup>-2</sup> day<sup>-1</sup> (**Figure 5A** and **Table 5**). UBC showed a decline in PO<sub>4</sub>-P removal when HLR was increased from 56 to 74 L m<sup>-2</sup> day<sup>-1</sup> (**Figure 5A**). Another decline in removal in UBC (from 46 to 27%) was observed when HLR was decreased from 112 to 74 L m<sup>-2</sup> day<sup>-1</sup>. In the CBC filter, increasing the HLR from 74 to 112 L m<sup>-2</sup> day<sup>-1</sup> enhanced PO<sub>4</sub>-P removal and CBC showed a decline (from 87%

to 71%) in PO<sub>4</sub>-P removal when HLR decreased from 112 to 74 L m<sup>-2</sup> day<sup>-1</sup> (**Figure 5B**).

The average percentage of removal of PO<sub>4</sub>-P in the FBC filter was not influenced by HLR (96% for all HLRs) (**Table 5** and **Figure 5C**). The trend in PO<sub>4</sub>-P removal in the PBC filter in response to changes in HLR was similar to that observed for UBC, but the levels of removal were higher in PBC (42 ± 40, 18 ± 78 and 29 ± 76% for HLR-56, HLR-74, and HLR-12, respectively) (**Figure 5D** and **Table 5**).

## Response of Filters to Increasing Phosphate Loading Rate

The average amount of  $\text{PO}_4\text{-P}$  retained in the media, increased as response to increase in PLR for all filters (Figure 6). Regarding  $\text{PO}_4\text{-P}$  removal in UBC as function of time, intermediate removal (~60%) was observed at the beginning of PLR-194, PLR-652, and PLR-1715, after which it then declined over time (Supplementary Figure S4A). For CBC, the average removal of  $\text{PO}_4\text{-P}$  decreased from 72% at PLR-194 to ~40% at PLR-324 and PLR-1715 (Supplementary Figure S4B).

In contrast, FBC showed high average removal of  $\text{PO}_4\text{-P}$  (>99%) at all PLRs until week 5 in PLR-1715, when removal began to decline (Supplementary Figure S4C). The average removal of  $\text{PO}_4\text{-P}$  in PBC was around 57% at PLR-194 to PLR-653, but declined drastically in PLR-1715 to reach 30% (Supplementary Figure S4D).

## DISCUSSION

### Adsorption Capacity of UBC, CBC, FBC, and PBC

In the batch adsorption experiment, the four biochar types were shaken with solutions of five different  $\text{PO}_4\text{-P}$  concentrations. CBC showed greatest P adsorption capacity, PBC and FBC both had lower but similar adsorption, and untreated biochar (UBC) adsorbed least P. The shape of the adsorption isotherm for CBC (Figure 3) showed that when the equilibrium concentrations

were low, the increase in equilibrium adsorption was also low. This may indicate involvement of dissolved organic compounds in P adsorption at low concentrations (Essington, 2004). The Freundlich model best fitted  $\text{PO}_4\text{-P}$  adsorption to CBC and PBC biochars, which means the adsorption to these materials can best be described as non-uniform. Adsorption to FBC biochar correlated better with the Langmuir adsorption model, which indicates that their adsorption can be modeled as homogeneous and in a monolayer over the biochar surface. Similarly, Li et al. (2016) found that P removal using wheat straw biochar impregnated with  $\text{FeCl}_3$  fitted well to a Langmuir model. In contrast, Chen et al. (2011) found that P adsorption by untreated and magnetite-coated biochar made from orange peel fitted the Freundlich model better.

The Langmuir adsorption constant  $k_F$  was higher for adsorption on PBC than for the other biochar types. This indicates that the affinity between P and PBC was highest for this material. The Langmuir maximum adsorption  $Q_m$  for CBC was negative, which is unrealistic, indicating that this model was not suitable for describing adsorption on CBC (Table 4). FBC had the highest  $Q_m$  ( $3.2 \text{ mg g}^{-1}$ ), but this is still lower than the  $16.58 \text{ mg g}^{-1}$  reported by Liu et al. (2015) for Fe-impregnated biochar made from wheat straw. The biochar in the study by Li et al. (2016) had smaller-diameter particles than the biochar used in this experiment (<1 mm compared with 1–7 mm) and higher iron to biochar ratio (0.7 compared with 0.3), which can explain the difference. The maximum adsorption capacity obtained in column filters (1.5, 4.02, 6.41, and  $2.75 \text{ mg g}^{-1}$ , for UBC, CBC,

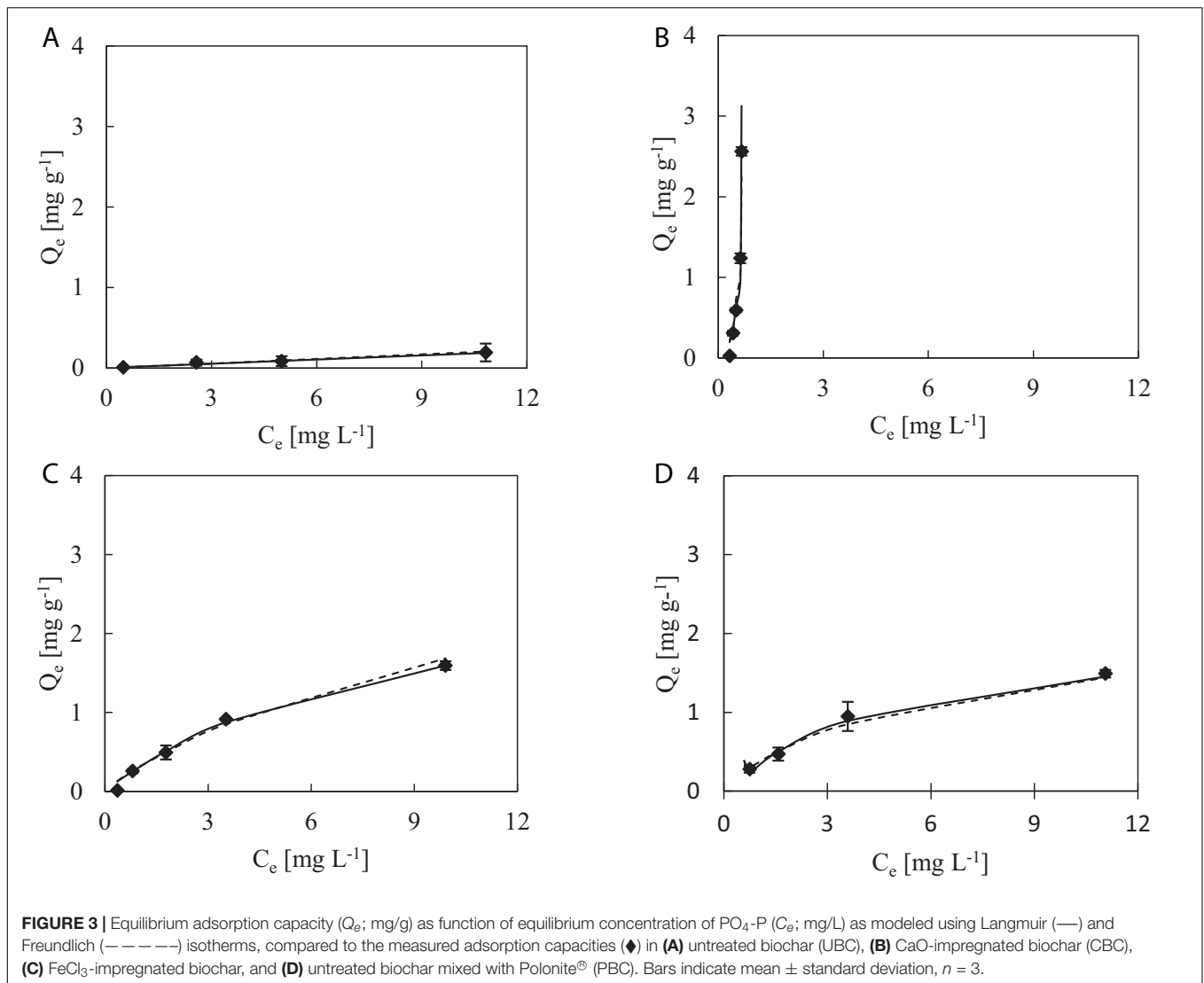
**TABLE 3** | Mineral content of biochar surfaces characterized using X-ray diffraction analysis.

Sample	Minerals	%	Sample	Minerals	%
Biochar untreated	Quartz	56	Biochar untreated, used for w/w filtration	Quartz	52
	Albite	27		Albite	26
	Microcline	17		Microcline	22
Biochar + CaO	Quartz	46	Biochar + CaO used for w/w filtration	Quartz	48
	Calcite	54		Albite	27
Biochar treated with $\text{FeCl}_3$	Quartz	44		Biochar + $\text{FeCl}_3$ used for w/w filtration	Microcline
	Akaganeite	32	Quartz		32
	Albite	24	Akaganeite		26
		Monalbite	24		
Polonite	Quartz	52	Biochar + Polonite used for w/w filtration	Albite	18
	Calcite	25		Quartz	61
	Wollastonite	23		Anorthite	32
		Orthoclase		7	

**TABLE 4** | Langmuir and Freundlich model parameters (mean  $\pm$  standard deviation,  $n = 3$ ) for untreated biochar (UBC), CaO-impregnated biochar (CBC),  $\text{FeCl}_3$ -impregnated biochar, and untreated biochar mixed with Polonite® (PBC).

Material	Langmuir model parameters			Freundlich model parameters		
	$Q_m$ ( $\text{mg g}^{-1}$ )	$k_L$ ( $\text{L mg}^{-1}$ )	$R^2$	$n$	$k_F$ ( $\text{L g}^{-1}$ )	$R^2$
UBC	$1.53 \pm 2.4$	$0.004 \pm 0.04$	$0.973 \pm 0.48$	$0.98 \pm 0.12$	$0.02 \pm 0.01$	$0.964 \pm 0.17$
CBC	–	–	–	–	–	–
FBC	$3.21 \pm 0.01$	$0.11 \pm 0.01$	$0.997 \pm 0.09$	$1.29 \pm 0.13$	$0.32 \pm 0.02$	$0.993 \pm 0.49$
PBC	$2.42 \pm 0.47$	$0.21 \pm 0.17$	$0.957 \pm 0.27$	$1.68 \pm 0.36$	$0.40 \pm 0.13$	$0.959 \pm 0.47$

Higher  $R^2$  value indicate better fit. –, the CBC did not reach equilibrium state during the experiment and therefore the adsorption models were not estimated.



FBC, and PBC, respectively) was higher in some cases (CBC and FBC) than in the batch experiment ( $1.53$ ,  $-0.41$ ,  $3.21 \pm 0.01$ , and  $2.42 \text{ mg g}^{-1}$ , respectively). Besides physical-chemical adsorption in the column filters, other factors may have contributed to this behavior, e.g., when PLR increased, more bacterial growth occurred in the filters and thus more  $PO_4$ -P was assimilated. The bacterial growth coupled with the competitive adsorption of organics can drastically affect the removal of phosphates (Dalahmeh et al., 2014). Moreover the complexation of organics with phosphates is also possible.

### Retention of Phosphate in Impregnated Biochar and Response to Loading Conditions

In filters designed for P removal, the capacity of the filter to retain  $PO_4$ -P depends on pH and the availability of surfaces rich in metal oxides such as Al-, Fe-, and Ca- oxides (Arias et al., 2001; Hylander et al., 2006). In this study, biochar filters impregnated

with Ca (CBC) and Fe (FBC) showed better removal of  $PO_4$ -P than UBC filters (UBC and PBC). The  $PO_4$ -P adsorbed to the FBC and CBC filters reacted with Fe and Ca minerals to form strong precipitates or surface complexes. The FBC filter maintained low pH ( $<4.5$ ) during the entire experimental period, indicating continuous formation of Fe oxides in FBC and hence enhanced  $PO_4$ -P adsorption to these oxides. This was confirmed by XRD tests of FBC surfaces after 100 weeks of operation, which showed a high content (26%) of akaganeite [a chloride-containing Fe (III) oxide-hydroxide mineral]. This indicated success in achieving long-lasting impregnation of biochar using  $FeCl_3$ . In contrast, with the CBC filter and its higher pH, the  $PO_4^{3-}$  ions formed complexes with Ca ions, so  $CaHPO_4 \cdot 2H_2O$  and  $Ca_4H(PO_4) \cdot 3H_2O$  could have been formed at the beginning of filter operation (US EPA, 2002). Adsorption of  $PO_4$ -P in CBC deteriorated over time. When the surface of the biochar was examined using XRD after 100 weeks of operation, CaO was not among the minerals deposited on the biochar. This shows that impregnation of biochar with CaO was reversed during operation



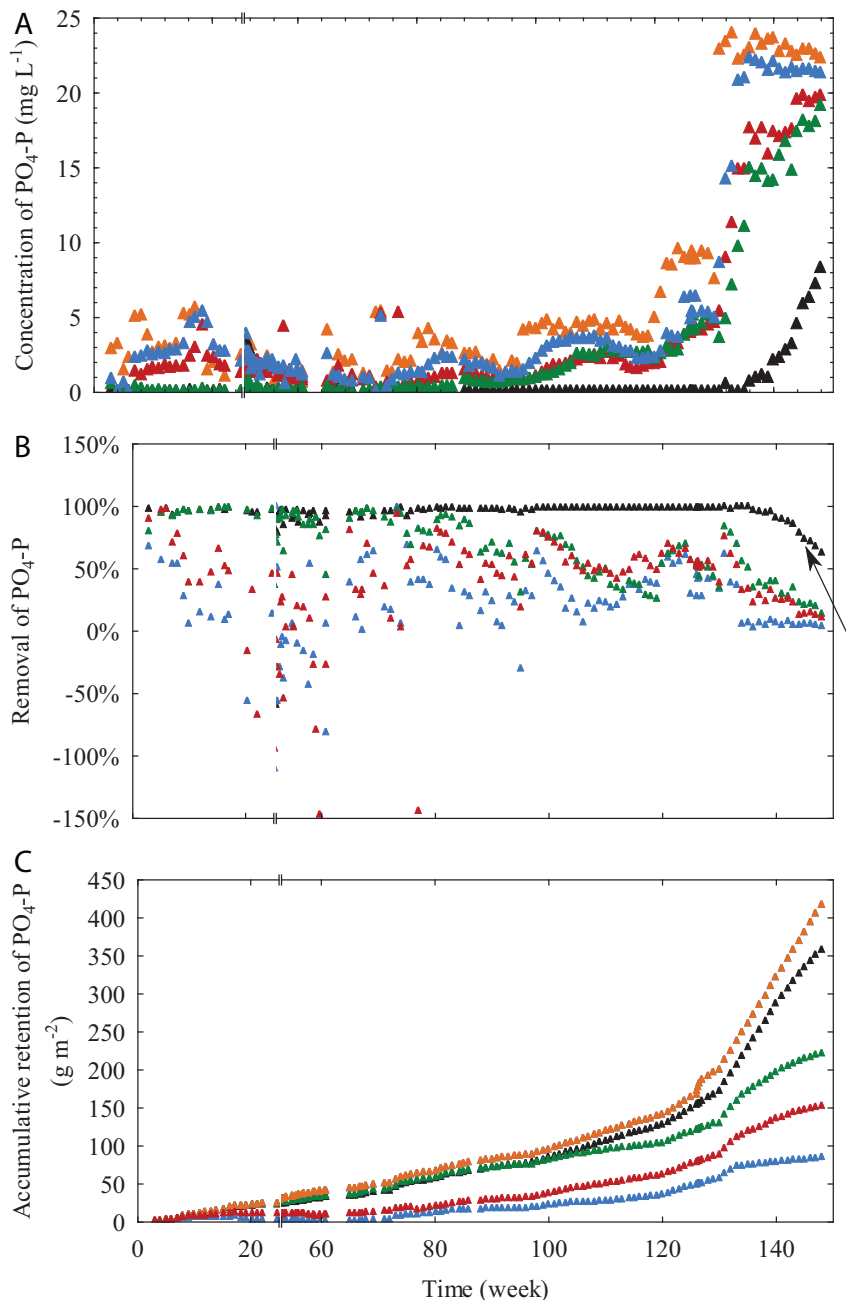


**FIGURE 4 | (A)** Concentration of phosphate-phosphorus ( $\text{PO}_4\text{-P}$ ) in the inflow to filters, **(B)** removal of  $\text{PO}_4\text{-P}$  in filters, and **(C)** cumulative amount of  $\text{PO}_4\text{-P}$  retained ( $\text{mg m}^{-2}$ ) from start to end of the experiment in: unimpregnated biochar filter (UBC; blue), CaO-impregnated biochar filter (CBC; green),  $\text{FeCl}_3$ -impregnated biochar filter (FBC; black), and biochar filter mixed with Polonite<sup>®</sup> (PBC; red). The orange line in panel (C) shows cumulative amount of  $\text{PO}_4\text{-P}$  ( $\text{g m}^{-2}$ ) applied to the filters.

of the filter. PBC showed less retention of  $\text{PO}_4\text{-P}$  than FBC and CBC, despite its high content of anorthite and orthoclase, which are known to bind phosphate (Figure 4). The amount of Polonite mixed with the biochar to produce PBC was only 30% of its weight and this was probably not enough to efficiently remove  $\text{PO}_4\text{-P}$  from wastewater over long periods. The UBC filter showed poor retention of  $\text{PO}_4\text{-P}$  and low removal (5–50%) during the

experiment, probably due to  $\text{PO}_4^{3+}$  assimilation to bacterial biofilms and to weak adsorption to silica and aluminum in the quartz, albite, and microcline deposited on the surface of UBC. These minerals likely originated from soil particles in wastewater.

Increasing the HLR from 56 to 74  $\text{L m}^{-2} \text{day}^{-1}$  decreased retention of  $\text{PO}_4\text{-P}$  in UBC and PBC. In fact, UBC experienced breakthrough at HLR-74 and  $\text{PO}_4\text{-P}$  desorbed/washed out from

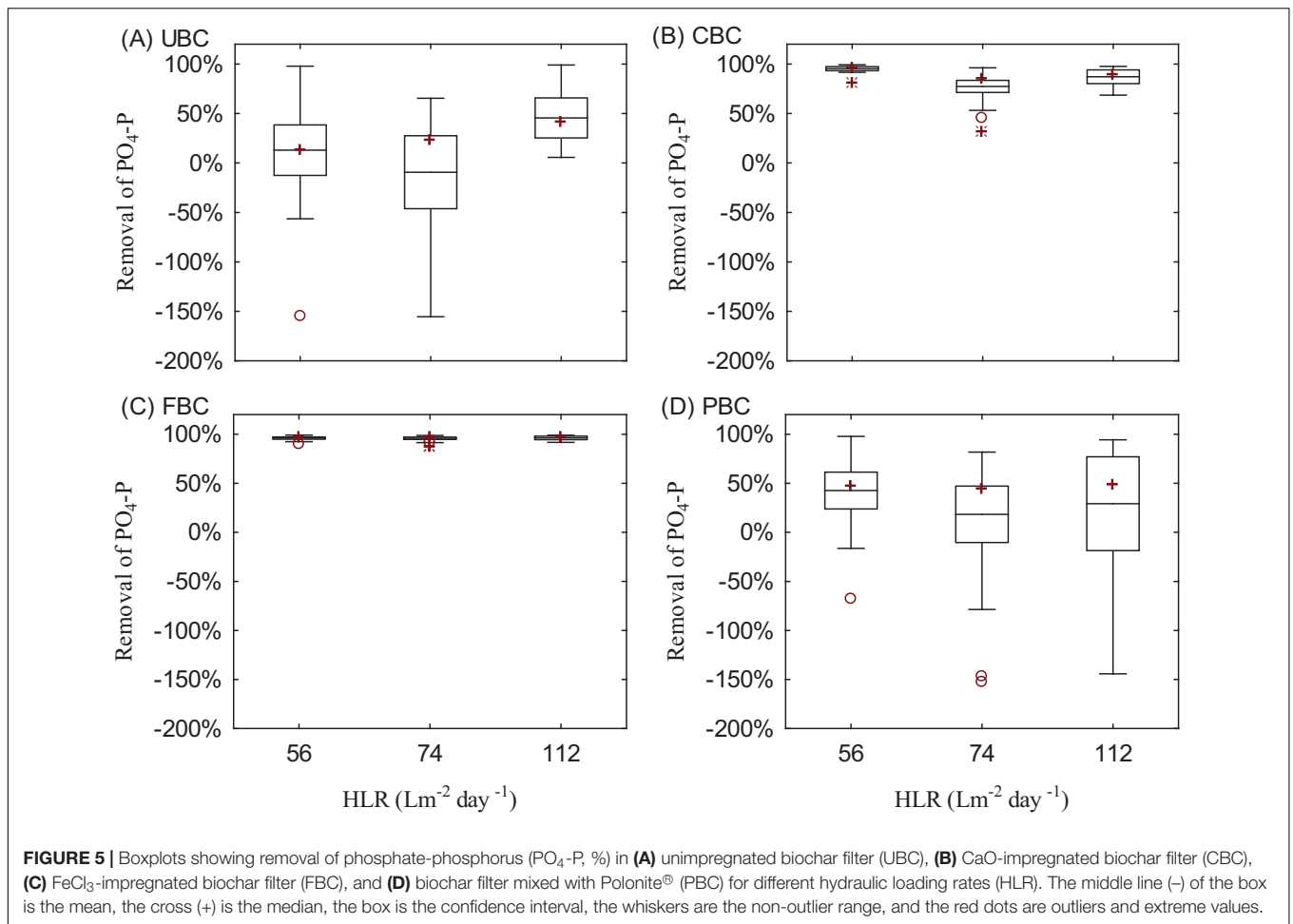


**FIGURE 5 |** Boxplots showing removal of phosphate-phosphorus (PO<sub>4</sub>-P, %) in (A) unimpregnated biochar filter (UBC), (B) CaO-impregnated biochar filter (CBC), (C) FeCl<sub>3</sub>-impregnated biochar filter (FBC), and (D) biochar filter mixed with Polonite® (PBC) for different hydraulic loading rates (HLR). The middle line (–) of the box is the mean, the cross (+) is the median, the box is the confidence interval, the whiskers are the non-outlier range, and the red dots are outliers and extreme values.

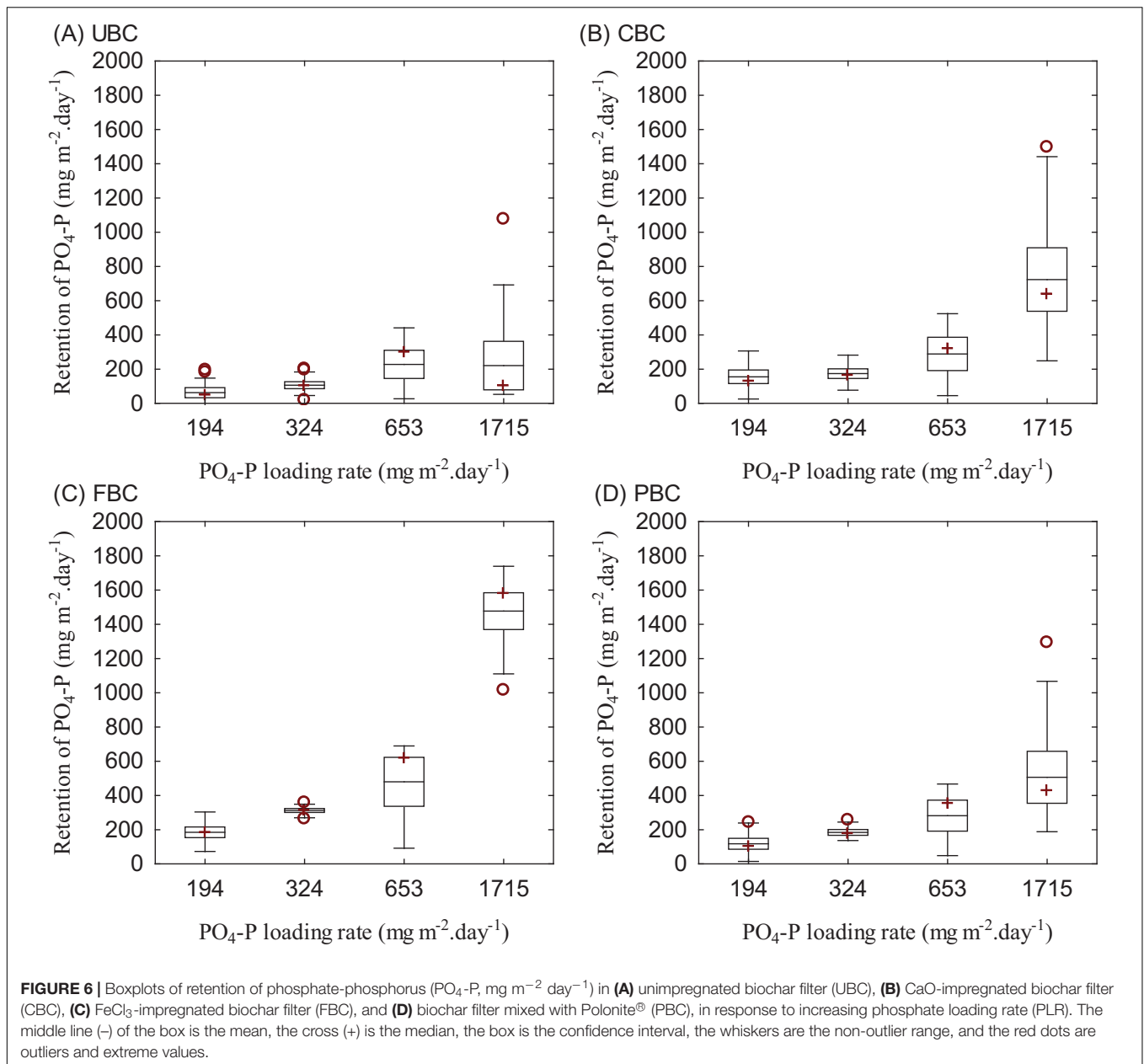
**TABLE 5 |** Concentrations of phosphate-phosphorus (PO<sub>4</sub>-P) in filter inflow and outflow, PO<sub>4</sub>-P retention (mg m<sup>-2</sup> day<sup>-1</sup>) and PO<sub>4</sub>-P removal in the unimpregnated biochar filter (UBC), CaO-impregnated biochar filter (CBC), FeCl<sub>3</sub>-impregnated biochar filter (FBC), and biochar filter mixed with Polonite® (PBC) at different hydraulic loading rates (HLR).

	Period	No. of weeks	HLR (L m <sup>2</sup> .day <sup>-1</sup> )	Concentration of PO <sub>4</sub> -P (mg L <sup>-1</sup> )	PLR and PO <sub>4</sub> -P retention (mg m <sup>2</sup> .day <sup>-1</sup> )	Removal of PO <sub>4</sub> -P (%)
Inflow	HLR-56	33	56	2.99 ± 1.33	167 ± 174 <sup>1</sup>	
	HLR-74	30	74	2.04 ± 1.08	152 ± 80 <sup>2</sup>	
	HLR-112	10	112	2.43 ± 1.60	271 ± 178	
UBC	HLR-56	33	112	2.53 ± 1.36	19 ± 102 <sup>1</sup>	13 ± 53
	HLR-74	30	74	1.64 ± 0.47	30 ± 71 <sup>2</sup>	-9 ± 100
	HLR-112	10	112	1.24 ± 0.14	134 ± 169	46 ± 28
CBC	HLR-56	33	74	0.12 ± 0.12	149 ± 93 <sup>1</sup>	95 ± 4
	HLR-74	30	112	0.41 ± 0.29	127 ± 80 <sup>2</sup>	77 ± 17
	HLR-112	10	74	0.24 ± 0.14	255 ± 187	87 ± 10
FBC	HLR-56	33	112	0.10 ± 0.07	140 ± 86 <sup>1</sup>	96 ± 2
	HLR-74	30	74	0.06 ± 0.04	143 ± 77 <sup>2</sup>	96 ± 3
	HLR-112	10	112	0.07 ± 0.04	257 ± 174	96 ± 3
PBC	HLR-56	33	74	1.63 ± 0.93	63 ± 101 <sup>1</sup>	42 ± 40
	HLR-74	30	112	1.16 ± 0.66	68 ± 99 <sup>2</sup>	18 ± 78
	HLR-112	10	74	1.64 ± 1.93	88 ± 218	29 ± 67

PLR, phosphorus loading rate.

<sup>1</sup>This loading period included the start-up and restart of the filter after reaching stable state.

<sup>2</sup>Average loading conditions during the periods HLR74-1 and HLR74-2.



the filter, indicating low robustness of UBC to sudden increases in HLR (Figure 5). The PBC filter did not show breakthrough when the HLR increased, but the removal rate of  $\text{PO}_4\text{-P}$  decreased substantially (from 42% to 18%). High hydraulic loads increase the infiltration rate and thereby reduce exchanges between mobile water in macropores and water retained in micropores (Boller et al., 1993). When HLR increases, the contact time between  $\text{PO}_4\text{-P}$  and the filter medium decreases and less adsorption occurs. For CBC, the first increase in HLR (HLR-56 to HLR-74) enhanced removal of  $\text{PO}_4\text{-P}$  due to enhanced surface wetting, and hence more  $\text{PO}_4\text{-P}$  reaching CaO hidden in biochar particles. However, when HLR-74 increased to HLR-112, removal of  $\text{PO}_4\text{-P}$  declined due to the washing-out of retained  $\text{PO}_4\text{-P}$ . Calcium is also likely to have been washed off the biochar surface in CBC when the

HLR increased, and hence less  $\text{PO}_4\text{-P}$  could be bound to CaO. This was confirmed by XRD analysis after HLR-112, in which CaO could not be detected in the CBC material. FBC was not influenced by HLR, because  $\text{PO}_4\text{-P}$  was mostly removed by chemical adsorption, in which the bonds between the  $\text{PO}_4$  and iron oxides are strong. Leaching of  $\text{PO}_4\text{-P}$  in this form will be triggered by e.g., changes in pH or oxidation-reduction (redox) potential. During the entire HLR trials, the pH in the FBC treatment was about 4 SU, with very low fluctuations.

With all filters except FBC, adsorption (retention) of  $\text{PO}_4\text{-P}$  in the filters increased as the PLR increased (Figure 6 and Supplementary Figure S4). This was due to UBC, CBC, and PBC developing new equilibrium conditions each time the PLR changed. This behavior was also observed in the batch adsorption

**TABLE 6** | Estimated service life<sup>1</sup> (in months) of unimpregnated biochar filter (UBC), CaO-impregnated biochar filter (CBC), FeCl<sub>3</sub>-impregnated biochar filter (FBC), and biochar filter mixed with Polonite® (PBC) under different phosphorus loading rates (PLR) at a fixed hydraulic loading rate of 74 L m<sup>-2</sup>.

Concentration of PO <sub>4</sub> -P (mg L <sup>-1</sup> )	PLR (mg m <sup>-2</sup> day <sup>-1</sup> )	Service life (months)			
		UBC	CBC	FBC <sup>2</sup>	PBC
2.6	194	–	15	58	–
4.4	324	–	9	35	–
8.8	652	–	4	17	–
23.2	1715	–	2	6	–

<sup>1</sup>Service life estimated as overall PO<sub>4</sub>-P retention (mg m<sup>-2</sup>) divided by PLR (mg m<sup>-2</sup>). Overall PO<sub>4</sub>-P retention was estimated as the cumulative amount of PO<sub>4</sub>-P retained in filters until they removed ≤70% of applied PO<sub>4</sub>-P. The CBC filter reached this limit after 1.65 years and FBC after 2.75 years.

trial, in which the increase in equilibrium concentrations ( $C_e$ ) resulted in an increase in P adsorbed on the surface. Moreover, the average concentration of PO<sub>4</sub>-P in the outflow increased in response to increasing PLR. At the beginning of each PLR trial, the concentration of PO<sub>4</sub>-P in the outflow from UBC, CBC, and PBC was initially low and increased with time, which indicated that PO<sub>4</sub>-P removal was high at the beginning of each PLR trial and decreased thereafter (**Supplementary Figure S4**). However, this was due to old water with low levels of PO<sub>4</sub>-P draining from the filters for several days after the onset of the new PLR. The hydraulic retention times were not determined for these filters.

In contrast, FBC maintained low PO<sub>4</sub>-P concentrations (<0.05 mg L<sup>-1</sup>) in outflow at high and low PLR (194–1715 g m<sup>2</sup> L<sup>-1</sup> day<sup>-1</sup>). This indicates that the adsorption capacity of the FBC material was mainly limited by chemical adsorption of PO<sub>4</sub> onto Fe oxides available on the surface of the filter. Removal of PO<sub>4</sub>-P declined in FBC at PLR-1715 and this was accompanied by an increase in pH from 4–4.5 to 5.0–5.4 SU, which showed that Fe oxides in FBC started to be consumed after formation of FeOOH-PO<sub>4</sub>. Siwek et al. (2019) reported that, with increasing pH, the sorption affinity of Fe compounds to PO<sub>4</sub><sup>3+</sup> drops, whereas the solubility of their combinations with P increases. The same study reported the optimal pH for creating durable complexes of FeOOH-PO<sub>4</sub> is below 5–7.

In general, PO<sub>4</sub>-P retention capacity was highest in FBC and lowest in UBC, with the filters following the order FBC>CBC>PBC>UBC, with overall PO<sub>4</sub>-P retention of 358.36, 221.75, 152.36, and 84.75 g m<sup>-2</sup>, respectively. Based on retention capacities, it was possible to estimate the service life of the FBC filter for different concentrations of PO<sub>4</sub>-P in wastewater (**Table 6**). The service life defined here is the time during which a filter can be successfully used to remove >70% of PO<sub>4</sub>-P from wastewater. This threshold was chosen because the Swedish regulations require 70% removal of PO<sub>4</sub>-P in areas classified as non-sensitive recipients (Havs- och vattenmyndighetens, 2016). Theoretically, having a low concentration (<2.6 mg L<sup>-1</sup>) of PO<sub>4</sub>-P in wastewater would allow the FBC filter to remain active for about 4.8 years and CBC to remain active for 1.25 years,

before their PO<sub>4</sub>-P removal declined to <70%. The wastewater in OWTS usually contains high concentrations (6–12 mg L<sup>-1</sup>) of PO<sub>4</sub>-P. If a FBC filter is used to treat wastewater without any pre-treatment (i.e., average PO<sub>4</sub>-P concentration 8.8 mg L<sup>-1</sup>), its service life may decline to 17 months, after which it may fail to meet the 70% PO<sub>4</sub>-P removal limit. The service life of UBC and PBC could not be estimated for the 70% removal limit, because these filters did not achieve efficient removal at the start of filter operation.

The column filters received wastewater, with all ingredients included (solids, organics, nutrient, micropollutants, etc.). It is likely that some of these elements might adsorb to biochar (e.g., NH<sub>4</sub>, pharmaceuticals, bacteria, viruses, and heavy metals), competing for removal of PO<sub>4</sub>-P. Biochar impregnated with Fe (FBC) can apparently be an effective filter material for removal of PO<sub>4</sub>-P from wastewater in OWTS. However, in full-scale implementation, it is recommended to use the FBC filter as a final treatment (or post-treatment) step for removal of PO<sub>4</sub>-P after organic matter and other competing elements have been removed from wastewater. This is likely to ensure effective utilization of the impregnated surfaces during planned use and to elongate the service life of the filter.

## CONCLUSION

1. The Freundlich model best fitted PO<sub>4</sub>-P adsorption to biochar mixed with Polonite (PBC), while adsorption to iron-impregnated filter material (FBC) biochar correlated better with the Langmuir adsorption model.
2. The enrichment of the FBC and CBC with Fe<sup>+3</sup> and Ca<sup>+2</sup> lead to effective adsorption of PO<sub>4</sub>-P through formation of strong precipitates and surface complexes.
3. FBC showed the best performance in phosphorus removal from wastewater. FBC showed high phosphate adsorption capacity and can achieve high retention over long periods, especially if wastewater contains <3 mg PO<sub>4</sub>-P L<sup>-1</sup>. This filter was robust and not sensitive to changes in hydraulic loading rate or phosphorus loading rate.
4. It is recommended that iron-impregnated biochar is used in a separate phosphorus filter module (post-treatment step) after organic matter and solids are removed from wastewater. With this approach, all adsorption sites on the impregnated biochar material will be available for phosphate removal.

## DATA AVAILABILITY STATEMENT

The datasets generated for this study are available on request to the corresponding author.

## AUTHOR CONTRIBUTIONS

SD and YS collected the data and wrote the article. MJ did FTIR analyses and revised the article. LH did the pyrolyses of biochar

and revised the article. GD did the SEM analyses and IH did the XRD analyses. All authors contributed to the article and approved the submitted version.

## FUNDING

This work was funded by the Swedish Agency for Water and Marine Management (Havs- och vattenmyndigheten) (Grant Number 864/2017), the Swedish Foundation for international cooperation in research and education (Grant Number PT2016–6875), Swedish research council for sustainable development (FORMAS) (Grant Numbers 2018-00261 and 2019-01257).

## ACKNOWLEDGMENTS

We gratefully acknowledge Almoayed Assayed and Anas Al-Mustafa for their efforts in the laboratory work.

## REFERENCES

- Agrafioti, E., Kalderis, D., and Diamadopoulos, E. (2014). Ca and Fe modified biochars as adsorbents of arsenic and chromium in aqueous solutions. *J. Environ. Manag.* 146, 444–450. doi: 10.1016/j.jenvman.2014.07.029
- Arias, C. A., Del Bubba, M., and Brix, H. (2001). Phosphorus removal by sands for use as media in subsurface flow constructed reed beds. *Water Res.* 35, 1159–1168. doi: 10.1016/S0043-1354(00)00368-7
- Berger, C. (2012). “Biochar and activated carbon filters for greywater treatment: comparison of organic matter and nutrient removal,” in *Energy and Technology*, (Uppsala: Swedish University of Agricultural Sciences).
- Boller, M., Schwager, A., Eugster, J., and Mottier, V. (1993). Dynamic behavior of intermittent buried filters. *Water Sci. Technol.* 28, 99–107. doi: 10.2166/wst.1993.0213
- Chen, B., Chen, Z., and Lv, S. (2011). A novel magnetic biochar efficiently sorbs organic pollutants and phosphate. *Bioresour. Technol.* 102, 716–723. doi: 10.1016/j.biortech.2010.08.067
- Dalahmeh, S. (2016). *Capacity of Biochar Filters for Wastewater Treatment in Onsite Systems – Technical Report: Report 2016-90*. Gothenburg: Havs och vattenmyndighet.
- Dalahmeh, S. S., Pell, M., Hylander, L. D., Lalander, C., Vinnerås, B., and Jönsson, H. (2014). Effects of changing hydraulic and organic loading rates on pollutant reduction in bark, charcoal and sand filters treating greywater. *J. Environ. Manag.* 132, 338–345. doi: 10.1016/j.jenvman.2013.11.005
- Del Bubba, M., Arias, C. A., and Brix, H. (2003). Phosphorus adsorption maximum of sands for use as media in subsurface flow constructed reed beds as measured by the Langmuir isotherm. *Water Res.* 37, 3390–3400. doi: 10.1016/S0043-1354(03)00231-8
- Downie, A., Krosky, A., and Munroe, P. (2009). “Physical properties of biochar,” in *Biochar for Environmental Management Science and Technology*, eds J. Lehmann, and S. Joseph, (London: Earthscan).
- Essington, M. E. (2004). *Soil and Water Chemistry: An Integrative Approach*. Boca Raton: CRC Press LLC.
- Havs- och vattenmyndigheten, (2016). *Havs- Och Vattenmyndighetens Allmänna råd om små Avloppsanordningar för Hushålls- och Vattenmyndigheten*, (Ed.) H.-o. Vattenmyndigheten, Vol. 17. Gothenburg: Havs- och vattenmyndigheten.
- He, S., Zhong, L., Duan, J., Feng, Y., Yang, B., and Yang, L. (2017). Bioremediation of wastewater by iron oxide-biochar nanocomposites loaded with photosynthetic bacteria. *Front. Microbiol.* 8:823. doi: 10.3389/fmicb.2017.00823

## SUPPLEMENTARY MATERIAL

The Supplementary Material for this article can be found online at: <https://www.frontiersin.org/articles/10.3389/fenvs.2020.538539/full#supplementary-material>

**Supplementary Figure 1** | Scanning electron microscope images of (A) unimpregnated biochar filter (UBC), (B) CaO-impregnated biochar filter (CBC), (C) FeCl<sub>3</sub>-impregnated biochar filter (FBC), and (D) biochar filter mixed with Polonite® (PBC). All images are shown at 10 μm resolution except Polonite (20 μm).

**Supplementary Figure 2** | X-ray diffraction patterns of untreated biochar (UBC) and biochar impregnated with CaO (CBC), before and after use for wastewater filtration.

**Supplementary Figure 3** | X-ray diffraction patterns of biochar treated with FeCl<sub>3</sub> (FBC) and biochar mixed with Polonite, before and after use for wastewater filtration.

**Supplementary Figure 4** | Percentage removal of phosphate-phosphorus (PO<sub>4</sub>-P) in (A) unimpregnated biochar filter (UBC), (B) CaO-impregnated biochar filter (CBC), (C) FeCl<sub>3</sub>-impregnated biochar filter (FBC), and (D) biochar filter mixed with Polonite (PBC), as a function of time at P loading rate (PLR)-194 (●), PLR-324 (■), PLR-652 (▲) and PLR-1715 (◆).

- He, Z., Uchimiya, S. M., and Guo, M. (2016). “Production and characterization of biochar from agricultural by-products: overview and use of cotton biomass residues,” in *Agricultural and Environmental Applications of Biochar: Advances and Barriers*, eds M. Guo, Z. He, and S. M. Uchimiya, (Madison, WI: Soil Science Society of America, Inc).
- Heinonen-Tanski, H., and Matikka, V. (2017). Chemical and microbiological quality of effluents from different on-site wastewater treatment systems across Finland and Sweden. *Water* 9:47. doi: 10.3390/w9010047
- HELCOM, (2018). *State of the Baltic Sea – Second HELCOM Holistic Assessment 2011-2016*. Helsinki: HELCOM.
- Hylander, L. D., Kietlinska, A., Renman, G., and Simán, G. (2006). Phosphorus retention in filter materials for wastewater treatment and its subsequent suitability for plant production. *Bioresour. Technol.* 97, 914–921. doi: 10.1016/j.biortech.2005.04.026
- Jebrane, M., Terziev, N., and Heinmaa, I. (2017). Biobased and sustainable alternative route to long-chain cellulose esters. *Biomacromolecules* 18, 498–504. doi: 10.1021/acs.biomac.6b01584
- Jung, K.-W., Jeong, T.-U., Kang, H.-J., and Ahn, K.-H. (2016). Characteristics of biochar derived from marine macroalgae and fabrication of granular biochar by entrapment in calcium-alginate beads for phosphate removal from aqueous solution. *Bioresour. Technol.* 211, 108–116. doi: 10.1016/j.biortech.2016.03.066
- Li, J. H., Lv, G. H., Bai, W. B., Liu, Q., Zhang, Y. C., and Song, J. Q. (2016). Modification and use of biochar from wheat straw (*Triticum aestivum* L.) for nitrate and phosphate removal from water. *Desalination Water Treat.* 57, 4681–4693. doi: 10.1080/19443994.2014.994104
- Liu, P., Liu, W.-J., Jiang, H., Chen, J.-J., Li, W.-W., and Yu, H.-Q. (2012). Modification of bio-char derived from fast pyrolysis of biomass and its application in removal of tetracycline from aqueous solution. *Bioresour. Technol.* 121, 235–240. doi: 10.1016/j.biortech.2012.06.085
- Liu, F., Zuo, J., Chi, T., Wang, P., and Yang, B. (2015). Removing phosphorus from aqueous solutions by using iron-modified corn straw biochar. *Front. Environ. Sci. Eng.* 9, 1066–1075. doi: 10.1007/s11783-015-0769-y
- Mead, J. (1981). A comparison of the Langmuir, Freundlich and Temkin equations to describe phosphate adsorption properties of soils. *Soil Res.* 19, 333–342. doi: 10.1071/sr9810333
- Niwagaba, C. B., Dinno, P., Wamala, I., Dalahmeh, S. S., Lalander, C., and Jönsson, H. (2014). Experiences on the implementation of a pilot grey water treatment and reuse based system at a household in the slum of Kyebando-Kisalosaloo, Kampala. *J. Water Reuse Desal.* 4, 294–307. doi: 10.2166/wrd.2014.016
- Palm, O., Malmén, L., and Jönsson, H. (2002). *Robusta, Uthålliga små Avloppssystem*. Stockholm: Naturvårdsverket.

- Ren, J., Li, N., Li, L., An, J.-K., Zhao, L., and Ren, N.-Q. (2015). Granulation and ferric oxides loading enable biochar derived from cotton stalk to remove phosphate from water. *Bioresour. Technol.* 178, 119–125. doi: 10.1016/j.biortech.2014.09.071
- Renman, A., and Renman, G. (2010). Long-term phosphate removal by the calcium-silicate material Polonite in wastewater filtration systems. *Chemosphere* 79, 659–664. doi: 10.1016/j.chemosphere.2010.02.035
- Schellenger, F. L., and Hellweger, F. L. (2019). Phosphorus loading from onsite wastewater systems to a lake (at long time scales). *Lake Reserv. Manag.* 35, 90–101. doi: 10.1080/10402381.2018.1541031
- Siwek, H., Bartkowiak, A., and Włodarczyk, M. (2019). Adsorption of phosphates from aqueous solutions on alginate/goethite hydrogel composite. *Water* 11:633. doi: 10.3390/w11040633
- Smith, V. H. (2003). Eutrophication of freshwater and coastal marine ecosystems: a global problem. *Environ. Sci. Pollut. Res.* 10, 126–139.
- US EPA, (2002). Onsite Wastewater Treatment Systems Manual. EPA/625/R-00/008. Washington, DC: United States Environmental Protection Agency.
- Conflict of Interest:** The authors declare that the research was conducted in the absence of any commercial or financial relationships that could be construed as a potential conflict of interest.

Copyright © 2020 Dalahmeh, Stenström, Jebrane, Hylander, Daniel and Heinmaa. This is an open-access article distributed under the terms of the Creative Commons Attribution License (CC BY). The use, distribution or reproduction in other forums is permitted, provided the original author(s) and the copyright owner(s) are credited and that the original publication in this journal is cited, in accordance with accepted academic practice. No use, distribution or reproduction is permitted which does not comply with these terms.